Enzyme Models

DOI: 10.1002/anie.200803939

Synthetic Support of De Novo Design: Sterically Bulky [FeFe]-Hydrogenase Models**

*Michael L. Singleton, Nattamai Bhuvanesh, Joseph H. Reibenspies, and Marcetta Y. Darensbourg**

Small-molecule models of the active site of [FeFe] hydrogenase (H_2ase)[1] are synthetic targets for the possibility that they might be adsorbed onto solid supports, such as graphite, and used in the construction of electrodes to be used in H^+ reduction and H_2 oxidation, as a replacement for platinum electrodes.[2] A distinct structural disparity between the most obvious precursor to models of the two iron subsites of the H cluster, the classic organoiron complex, $[(\mu\text{-}S(CH_2)_3S\text{-})\{Fe^I(CO)_3\}_2]$,[3,4] (Figure 1, **B**), and the enzyme active site (EAS) structure (Figure 1, **A**), is the orientation of the edge-sharing square-pyramidal arrangements, that define the coordination sphere about each iron. The EAS, exhibiting a "rotated" edge-bridged square-pyramid/inverted square-pyramid geometry around the iron centers, has been structurally characterized in a mixed-valent, Fe^IFe^{II} oxidation state.[1] However, the structure is apparently retained throughout the redox states of the catalytic cycle including the reduced Fe^IFe^I form.[7] That the reduced form does not rearrange to the more symmetrical conformer, as found in **B**, is seemingly enforced by the secondary coordination sphere (hydrogen bonding of the cyanide groups to nearby lysine or serine residues) and steric effects from the surrounding protein matrix (the proximity of a phenylalanine and several other hydrophobic residues to the "open" or rotated site).[8] The significance of the rotated structure apparently lies in the requirement of an open site on the catalytically active iron for the binding of H_2 or H^- in a terminal position.[9]

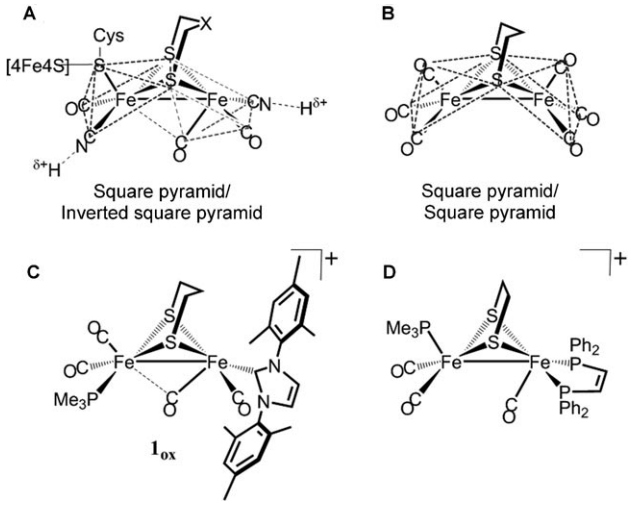

Figure 1. **A**) The enzyme active site of [FeFe]-hydrogenase, showing the "rotated" geometry.[1] **B**) Parent model complex $[(\mu\text{-pdt})\{Fe(CO)_3\}_2]$.[4] **C**, **D**) Recently reported model complexes with similar geometries to the [FeFe]-hydrogenase active site.[5,6]

Since the elucidation of the [FeFe] H_2ase EAS structure, several hundred small-molecule models based on the simple complex **B** ($[(\mu\text{-SRS})\{Fe(CO)_3\}_2]$, R = bridging group) have been synthesized, in attempts to mimic both the structure and function of the enzyme. With an inestimable number of permutations involving different CO-ligand substitutions, isomeric forms, and bridging "R" substituents,[10] the use of theoretical studies to explore the unique features of the EAS as well as to limit the optimal synthetic targets has proven to be a valuable strategy for our work. Density functional (DFT) calculations by Tye et al. helped to define the criteria for reproducing the geometry found in the two-iron subsites of [FeFe] H_2ase.[11] The rotated geometry (a transition state) of $[(\mu\text{-SRS})\{Fe^I(CO)_3\}_2]$ was found to be stabilized by substitution of CO by more electron-donating ligands, such as cyanide or phosphine, particularly when in the apical position of the unrotated $Fe(CO)_2L$ moiety and *trans* to the semibridging CO arising from full rotation (see Figure 1). Both one-electron reduction and oxidation decrease the Fe^I–Fe^I bond order to $^1/_2$, and the transition state that represents the rotated form of Fe^IFe^0 is some 4 kcal mol^{-1} lower in energy than that arising from the Fe^IFe^I complex. Unexpectedly the ground state of the Fe^IFe^{II} complex is, in some cases, predicted to be stable in the rotated form.[11,12] Such computations presaged the synthesis of the Fe^IFe^{II} complexes **C** (complex $\mathbf{1_{ox}}$, bearing a bulky N-heterocyclic carbene (NHC) ligand, 1,3-bis(2,4,6-trimethylphenyl)imidazol-2-ylidene, IMes) and **D** (Figure 1). These complexes are thermally sensitive but sufficiently stable to permit characterization by X-ray crystallography as the first rotated structures in small-molecule models.[11,12] Notably, both $\mathbf{1_{ox}}$ and **D** have ligand-based arene groups, positioned to flank the open site on iron in the rotated unit, thus indicating the need for a steric effect to stabilize the rotated structure. Spin density computations suggest that the inverted square-pyramidal moiety incorporates d^7 Fe^I, whereas the unrotated group incorporates Fe^{II}.[13]

[*] M. L. Singleton, Dr. N. Bhuvanesh, Dr. J. H. Reibenspies, Prof. M. Y. Darensbourg
Department of Chemistry, Texas A&M University
College Station, TX 77843 USA
Fax: (+1) 979-845-0158
E-mail: marcetta@mail.chem.tamu.edu

[**] We acknowledge financial support from the National Science Foundation (CHE-0616695 and CHE-0541587) and the R. A. Welch Foundation (A-0924).

Supporting information for this article is available on the WWW under http://dx.doi.org/10.1002/anie.200803939.

DFT computations on the $Fe^{I}Fe^{I}$ complexes also revealed that steric bulk built into the bridgehead carbon of the S–S bridging ligand further stabilizes the higher-energy conformer, relative to the unrotated ground state.[11] In support of this prediction, we report herein that, even when small substituent ligands are used, steric bulk incorporated into the S–S bridging ligand permits access to a stable $Fe^{I}Fe^{II}$ derivative with a rotated geometry and a semibridging CO group, resembling the EAS.

The reaction of $[(\mu\text{-dmpdt})\{Fe(CO)_3\}_2]$ (dmpdt = 2,2-dimethyl-1,3-propanedithiolate)[14] with trimethylphosphine yields $[(\mu\text{-dmpdt})\{Fe(CO)_2PMe_3\}_2]$ (**2***), as dark red crystals in 60–70% yield (Scheme 1). Notably, infrared spectroscopy of **2*** gives $\tilde{\nu}$(CO) values nearly identical to those of $[(\mu\text{-pdt})\{Fe(CO)_2PMe_3\}_2]$ (**2**, pdt = 1,3-propanedithiolate), indicating that the electronic effect from bridgehead carbon substitution is insignificant.[15]

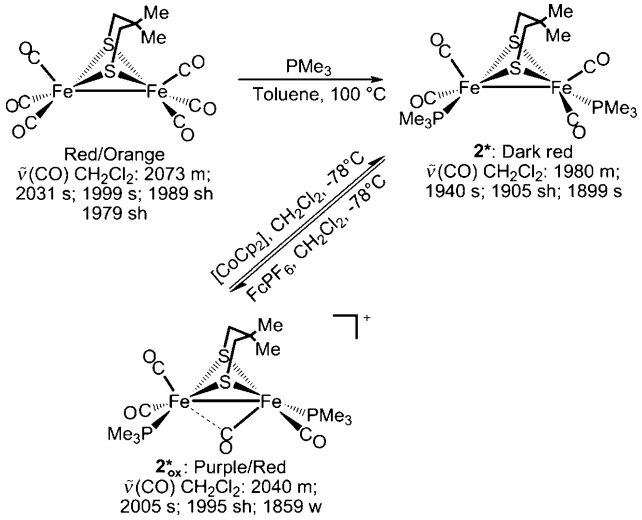

Scheme 1. Synthesis and $\tilde{\nu}$(CO) values (cm^{-1}, from infrared spectroscopy) of complexes **2*** and $(\mathbf{2^*_{ox}})PF_6$.

^{13}C NMR spectroscopic data show fluxionality in the S–S bridging ligand of **2*** and a similar low barrier to intramolecular CO site-exchange within the $Fe(CO)_2PMe_3$ units, ceasing at −90 °C. The molecular structure of **2***, determined by X-ray diffraction (Figure 2, inset) is largely typical of $[(\mu\text{-SRS})\{Fe(CO)_2L\}_2]$ complexes, albeit with a staggering of the $Fe(CO)_2PMe_3$ units, resulting in a C_{ap}-Fe-Fe′-C'_{ap} torsion angle of approximately 30° (about 20° greater than that of **2**).[15]

Cyclic voltammetry of complexes **1**, **2**, and **2*** (Figure 3) indicates that the bridgehead bulk in **2*** results in an anodic shift of the $Fe^{I}Fe^{I}/Fe^{II}Fe^{I}$ oxidation potential of approximately 240 mV, as compared to **2**.[16] The quasi-reversible oxidation event in **2** also becomes fully reversible in **2***. As the μ-dmpdt and μ-pdt ligands have similar electron-donating abilities,[14] the electrochemical differences can be attributed solely to the influence of the steric effect from the *gem*-dimethyl groups on **2***. Most importantly, the fully reversible redox event at −0.34 V (Figure 3a) suggests the possibility of bulk chemical oxidation and isolation of $\mathbf{2^*_{ox}}$ (Scheme 1).

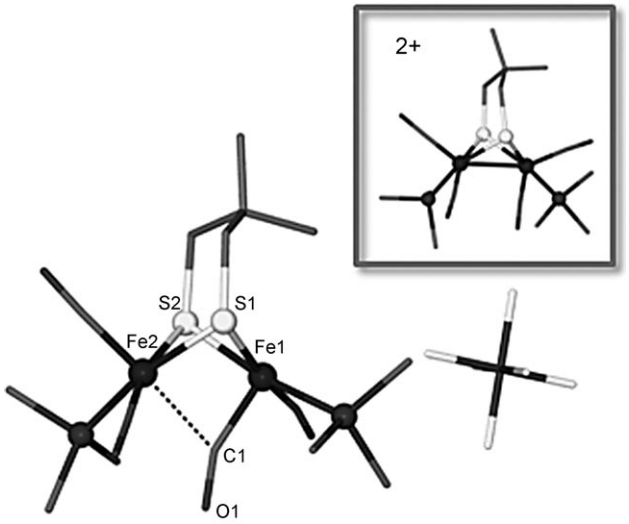

Figure 2. Ball-and-stick representation of the molecular structure of the cation $\mathbf{2^*_{ox}}$, and precursor **2*** (inset). Significant distances (Å) and angles (°) of $\mathbf{2^*_{ox}}$ and **2*** (square brackets): Fe1–Fe2 2.532(2) [2.569(1)], Fe1–C1 1.814(6), Fe2–C1 2.204(6), Fe1-C1-O1 146(4)°, Fe2-C1-O1 133(3). Flap angle = 123° [141°]. The "flap" angle refers to the angle between the mean planes comprising the three CH_2 units and that comprising of the two CH_2S units. A full listing of metric parameters is given in the Supporting Information.

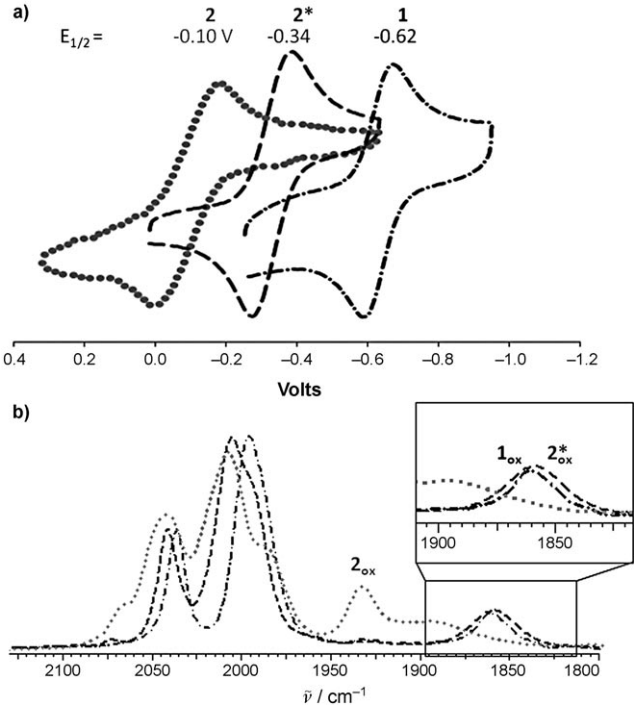

Figure 3. a) Cyclic voltammograms showing the $Fe^{I}Fe^{I}/Fe^{II}Fe^{I}$ redox events in **1**, **2**, and **2*** (2 mM in CH_2Cl_2, with 0.1 M nBu_4NBF_4 as electrolyte, scan rate: 200 $mV s^{-1}$). b) Comparison of the infrared spectra of $\mathbf{1_{ox}}$ (–•–•), $\mathbf{2_{ox}}$ (••••), and $\mathbf{2^*_{ox}}$ (-----) in the $\tilde{\nu}$(CO) region.

The IR spectral changes in $\tilde{\nu}$(CO), accompanying oxidation of **2***, include the appearance of a weak band at 1859 cm^{-1}, indicative of a bridging or semibridging CO

ligand (Figure 3b) similarly to that in $\mathbf{1}_{ox}$.[11] X-ray crystallographic studies of $\mathbf{2}^*_{ox}$ confirm the presence of this ligand (Figure 2). Crystals of $\mathbf{2}^*_{ox}$ were obtained from a concentrated dichloromethane solution, cooled in a Dewar flask with a thermal gradient from −15 °C to −78 °C. Notably, the CO ligand in the apical position of square-pyramidal Fe1 is bound in a nonlinear manner (Fe1-C1-O1 = 146(3)°). Furthermore, asymmetric Fe–C distances also indicate the semibridging character of the C1, which leads to a pseudo-6-coordinate octahedral geometry at Fe2. The Fe–Fe distance of 2.532(2) Å in cationic $\mathbf{2}^*_{ox}$ is slightly shorter than that in neutral **2***. Notably, the S to S linker of $\mathbf{2}^*_{ox}$ has a more acute "flap" angle (the angle between the mean planes comprising the three CH_2 units and that composed of the two CH_2S units) than the neutral Fe^IFe^I precursor **2***. Upon oxidation of **2*** to $\mathbf{2}^*_{ox}$, the flap angle decreases by 30°, in contrast to the oxidation of **1** to $\mathbf{1}_{ox}$, whereupon no significant change occurs (123.03° to 122.97°). There are no apparent intermolecular interactions that would influence the position of the bridgehead methyl substituents in $\mathbf{2}^*_{ox}$, whereas steric hindrance from the apical CO groups in the neutral precursor accounts for the greater flap angle of **2***.

DFT calculations presented further elucidation of the structure of $\mathbf{2}^*_{ox}$ (Figure 4, see the Supporting Information for full results of DFT calculations). The overlay of the DFT-optimized structure of the $\mathbf{2}^*_{ox}$ cation with that from the X-ray diffraction study shows a precise match of the $\{Fe_2S_2\}$ core and the semibridging CO ligand. As with $\mathbf{1}_{ox}$, unpaired spin density in the spin-density plot clearly indicates that the d^7 Fe^I exhibits rotated square-pyramidal geometry in $\mathbf{2}^*_{ox}$.

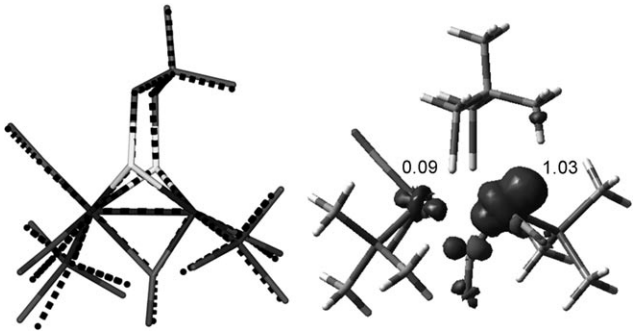

Figure 4. Left: Overlay of calculated structure (solid bonds) and the crystal structure (determined by X-ray diffraction, dashed bonds) of $\mathbf{2}^*_{ox}$. Right: Calculated spin-density plot showing the majority of the unpaired spin density on the rotated side of the complex. Mulliken atomic spin densities are indicated. The isodensity value for the spin density contour plot is 0.004.

Complex $\mathbf{2}^*_{ox}$ is EPR-active and shows a rhombic signal, i.e. the elements of the *g* tensor are all different, that is simulated as a single species with hyperfine coupling to a single nucleus (Figure 5). The *g* values (2.086, 2.025, and 2.007) are similar to those reported for both the EAS and previously reported models ($\mathbf{1}_{ox}$ and **D**, Figure 1).[5,6,17,18] Hyperfine coupling ($a \approx 25$) to only one of the PMe_3 ligands does not unambiguously identify the location of the unpaired electron in the $\mathbf{2}^*_{ox}$ complex. It does, however, provide further

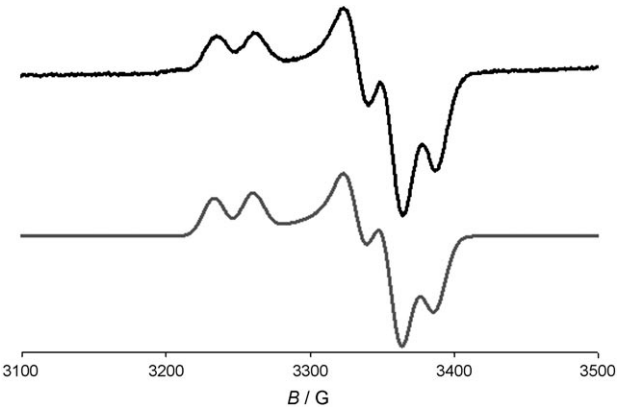

Figure 5. EPR spectrum of $\mathbf{2}_{ox}$ (top) and Simfonia simulation (bottom). *g* Values and ^{31}P super hyperfine coupling parameters (*a*): $g_1 = 2.086$, $a = 27.0$; $g_2 = 2.025$, $a = 25$; $g_3 = 2.007$, $a = 25$.

evidence that, in complex $\mathbf{1}_{ox}$, the rotated iron (that which bears the IMes ligand in $\mathbf{1}_{ox}$) is Fe^I, as no ^{31}P hyperfine coupling is seen in its EPR spectrum.[5] This result is also consistent with computational studies of both $\mathbf{1}_{ox}$ and $\mathbf{2}^*_{ox}$.[13]

Despite having a partially reversible $Fe^IFe^I/Fe^{II}Fe^I$ redox couple at 22 °C, the sterically unhindered complex **2** reacts with ferrocenium hexafluorophosphate ($FcPF_6$) at −78 °C to produce a highly unstable one-electron oxidized species, $\mathbf{2}_{ox}$, that is EPR-active. The spectrum obtained for this paramagnetic species is best simulated as axial, i.e., two of the three contributors to the *g* tensor are equal; however, the observed broadening and small values required for simulated result in a signal that is nearly isotropic.. The disparity between these values and those obtained for $\mathbf{2}^*_{ox}$ indicates structural differences, as also implied by the infrared spectroscopy, wherein for $\mathbf{2}^*_{ox}$ no signal indicative of a semibridging CO is detected in the region 1900–1800 cm^{-1} (Figure 3b). Such sensitivity to a seemingly minor change in the S to S bridging ligand is reminiscent of the delicate balance of steric effects from the NHC ligands, which are known to determine whether rotation occurs in a series of $[(\mu\text{-pdt})\{Fe(CO)_2PMe_3\}\{Fe(CO)_2NHC\}]^+$ complex cations.[12]

In summary, as predicted by de novo design,[11] the addition of steric bulk to the S to S bridging ligand in these diiron model complexes is sufficient to enforce a significant twist in the solid-state structure of **2***, facilitating the Fe^IFe^I/Fe^IFe^{II} oxidation and leading to the first structurally characterized [FeFe]-H_2ase EAS model complex that has a bridging CO and does not require sterically bulky ligands. EPR results and DFT calculations for $\mathbf{2}^*_{ox}$ indicate that the rotated half of this complex incorporates d^7 Fe^I, whereas the unrotated half contains the d^6 Fe^{II}. Studies on the complex $\mathbf{2}_{ox}$, lacking steric hindrance in either the substituent ligands or the S to S bridging ligand, give no evidence of a bridging CO. Its EPR spectrum indicates a substantially different electronic environment surrounds the unpaired electron. Thus, the need for steric bulk to stabilize the rotated form can be met by two structural motifs in the model complexes: appropriate bulk in the substituent ligands or in the S–S bridging ligand. To maintain this rotated structure, throughout the redox process

in the catalytic cycle of hydrogen production ($Fe^{I}Fe^{I}$) or uptake ($Fe^{II}Fe^{II}$), remains a formidable challenge.

Experimental Section

Synthesis of [(μ-dmpdt){$Fe(CO)_2PMe_3$}$_2$] (**2***): Under N_2 a solution of [(μ-dmpdt){$Fe(CO)_3$}$_2$] (0.500 g, 1.21 mmol) and PMe_3 (1 mL) in 100 mL toluene was heated to 100°C. The IR monitor showed complete reaction after 48 h. Complex **2*** was isolated in > 70% yield after solvent removal and recrystallization in MeOH. Crystals of X-ray quality were obtained from a concentrated MeOH solution stored at −4°C for 24 h.

Synthesis of [(μ-dmpdt){$Fe(CO)_2PMe_3$}$_2$]PF_6 (**2*$_{ox}$**): A solution of **2*** (0.051 g, 0.100 mmol in 10 mL of dichloromethane) was cooled to −78°C and added to a precooled test tube containing solid ferrocenium hexafluorophosphate. (0.033 g, 0.100 mmol). The reaction mixture was stirred for 10 min and then warmed to −42°C. Addition of 20 mL of precooled hexane (−78°C) gave the product as a purple-red precipitate. The supernatant was cannulated off and the product was washed with two (20 mL) portions of hexane precooled to −78°C. Yield: 0.49 mg (87%).X-ray quality crystals were obtained by transferring the CH_2Cl_2 reaction solution to a 12 mm diameter glass tube capped with a rubber septum. This was then stored in a Dewar flask filled halfway with ethylene glycol/$CO_{2(s)}$ and the rest of the way with crushed $CO_{2(s)}$. After 14 days, suitable crystals had formed. Further details and all characterizations are given in the Supporting Information.

X-ray crystallography: CCDC 698119 and 698120 contain the supplementary crystallographic data for this paper. These data can be obtained free of charge from The Cambridge Crystallographic Data Centre via www.ccdc.cam.ac.uk/data_request/cif

Received: August 8, 2008
Published online: October 27, 2008

Keywords: de novo design · enzyme models · hydrogenases · iron · steric hindrance

[1] Y. Nicolet, B. J. Lemon, J. C. Fontecilla-Camps, J. W. Peters, *Trends Biochem. Sci.* **2000**, *25*, 138.
[2] J. A. Cracknell, K. A. Vincent, F. Armstrong, *Chem. Rev.* **2008**, *108*, 2439.
[3] D. Seyferth, R. S. Henderson, L.-C. Song, *J. Organomet. Chem.* **1980**, *192*, C1.
[4] a) E. J. Lyon, I. P. Georgakaki, J. H. Reibenspies, M. Y. Darensbourg, *Angew. Chem.* **1999**, *111*, 3373; *Angew. Chem. Int. Ed.* **1999**, *38*, 3178.
[5] T. Liu, M. Y. Darensbourg, *J. Am. Chem. Soc.* **2007**, *129*, 7008.
[6] a) A. K. Justice, T. B. Rauchfuss, S. R. Wilson, *Angew. Chem.* **2007**, *119*, 6264; *Angew. Chem. Int. Ed.* **2007**, *46*, 6152; b) A. K. Justice, L. De Gioia, ; M. J. Nilges, T. B. Rauchfuss, S. R. Wilson, G. Zampella, *Inorg. Chem.* **2008**, *47*, 7405; M. J. Nilges, T. B. Rauchfuss, S. R. Wilson, G. Zampella, *Inorg. Chem.* **2008**, *47*, 7405.
[7] a) Y. Nicolet, A. L. De Lacey, X. Vernède, V. M. Fernandez, C .E. Hatchikian, J. C. Fontecilla-Camps, *J. Am. Chem. Soc.* **2001**, *123*, 1596; b) M. Y. Darensbourg, E. J. Lyon, X. Zhao, I. P. Georgakaki, *Proc. Natl. Acad. Sci. USA* **2003**, *100*, 3683.
[8] J. W. Peters, W. N. Lanzilotta, B. J. Lemon, L. C. Seefeldt, *Science* **1998**, *282*, 1853.
[9] a) B. E Barton, T. B. Rauchfuss, *Inorg. Chem.* **2008**, *47*, 2261; b) S. Ezzaher, J.-F. Capon, F. Gloaguen, F. Y. Petillon, P. Schollhammer, J. Talarmin, ; R. Pichon, N. Kervarec, *Inorg. Chem.* **2007**, *46*, 3426; R. Pichon, N. Kervarec, *Inorg. Chem.* **2007**, *46*, 3426.
[10] X. Zhao, I. P. Georgakaki, M. L. Miller, R. Mejia-Rodriguez, C. Chiang, M. Y. Darensbourg, *Inorg. Chem.* **2002**, *41*, 3917.
[11] J. W. Tye, M. B. Hall, M. Y. Darensbourg, *Inorg. Chem.* **2006**, *45*, 1552.
[12] C. M. Thomas, T. Liu, M. B. Hall, M. Y. Darensbourg, *Inorg. Chem.* **2008**, *47*, 7009.
[13] C. M. Thomas, M. Y. Darensbourg, M. B. Hall, *J. Biol. Inorg. Chem.* **2007**, *101*, 1752.
[14] M. L. Singleton, R. M. Jenkins, C. L. Klemashevich, M. Y. Darensbourg, *C. R. Chim.* **2008**, *11*, 861.
[15] X. Zhao. I. P. Georgakaki, M. L. Miller, J. C. Yarbrough, M. Y. Darensbourg, *J. Am. Chem. Soc.* **2001**, *123*, 9710.
[16] R. Mejia-Rodriguez, D. Chong, J. H. Reibenspies, M. P. Soriaga, M. Y. Darensbourg, *J. Am. Chem. Soc.* **2004**, *126*, 12004.
[17] B. Bennett, B. J. Lemon, J. W. Peters, *Biochemistry* **2000**, *39*, 7455.
[18] R. T. Baker, P. J. Krusic, J. C. Calabrese, D. C. Roe, *Organometallics* **1986**, *5*, 1506.

